UNIVERSITY OF PATRAS - SCHOOL OF ENGINEERING
DEPARTMENT OF ELECTRICAL AND COMPUTER ENGINEERING

ΠΑΝΕΠΙΣΤΗΜΙΟ ΠΑΤΡΩΝ
UNIVERSITY OF PATRAS

Division: Systems and Automatic Control

Thesis

of the student of the Department of Electrical and Computer Engineering of the School of Engineering of the University of Patras

Karadimos Alexios of Loukas

Student Number: 1046820

Subject

Robotic surgical tool manipulator - Recognition, control and manipulation of laparoscopic tools

Supervisor

Associate Professor Dr. Evangelos Dermatas

Co-Supervisor

Professor Dr. Anthony Tzes

Thesis Number:

Patras, 2020

ΠΙΣΤΟΠΟΙΗΣΗ

Πιστοποιείται ότι η διπλωματική εργασία με θέμα

Robotic surgical tool manipulator - Recognition, control and manipulation of laparoscopic tools

του φοιτητή του Τμήματος Ηλεκτρολόγων Μηχανικών και Τεχνολογίας Υπολογιστών

Karadimos Alexios of Loukas

(A.M.: 1046820)

παρουσιάστηκε δημόσια και εξετάστηκε στο τμήμα Ηλεκτρολόγων Μηχανικών και Τεχνολογίας Υπολογιστών στις

__/__/___

Ο Επιβλέπων

Ο Διευθυντής του Τομέα

Evangelos Dermatas
Associate Professor Dr.

Kazakos Demosthenes
Assistant Professor Dr.

CERTIFICATION

It is certified that the Thesis with Subject

Robotic surgical tool manipulator - Recognition, control and manipulation of laparoscopic tools

of the student of the Department of Electrical and Computer Engineering

Karadimos Alexios of Loukas

(R.N.: 1046820)

Was presented publicly and defended at the Department of Electrical and Computer Engineering at

__/__/___

The supervisor	The Director of the Division
Evangelos Dermatas	Kazakos Demosthenes
Associate Professor Dr.	*Assistant Professor Dr.*

Thesis details

Subject: **Robotic surgical tool manipulator - Recognition, control and manipulation of laparoscopic tools**

Student: **Karadimos Alexios of Loukas**

Supervising Team:
Associate Professor Dr. Evangelos Dermatas, University of Patras
Professor Dr. Anthony Tzes, NYU Abu Dhabi

Thesis research period:

Abstract

Sunt proident ut incididunt veniam ad excepteur aute nostrud. Anim nulla magna proident dolore non laboris deserunt irure. Aliqua velit quis labore quis nisi. Adipisicing amet dolor officia est ex nulla enim anim minim laboris nisi adipisicing cupidatat. Ut do consequat est ad sint dolore. Eiusmod ipsum nulla do aute culpa ad veniam eu in sunt qui laboris. Ea exercitation et quis fugiat.

Περίληψη

Sunt proident ut incididunt veniam ad excepteur aute nostrud. Anim nulla magna proident dolore non laboris deserunt irure. Aliqua velit quis labore quis nisi. Adipisicing amet dolor officia est ex nulla enim anim minim laboris nisi adipisicing cupidatat. Ut do consequat est ad sint dolore. Eiusmod ipsum nulla do aute culpa ad veniam eu in sunt qui laboris. Ea exercitation et quis fugiat.

Acknowledgements

Sunt proident ut incididunt veniam ad excepteur aute nostrud. Anim nulla magna proident dolore non laboris deserunt irure. Aliqua velit quis labore quis nisi. Adipisicing amet dolor officia est ex nulla enim anim minim laboris nisi adipisicing cupidatat. Ut do consequat est ad sint dolore. Eiusmod ipsum nulla do aute culpa ad veniam eu in sunt qui laboris. Ea exercitation et quis fugiat.

Contents

1 Introduction

1.1 Surgical robotics

1.1.1 Historical Overview of Surgical robotics

Surgical robotics is a field of Surgery where the surgeon operaties on the patient via a computer, specialised equipment and robotic arms, to which the surgical tools needed for the operation are attached. According to surgical bibliography, robotics and laparoscopic procedures are used in general surgery, cardiothoracic surgeries, colon surgeries, gynecology, neurosurgery and orthopedics.

Robotic mechanisms were first introduced in Medicine, in 1987 with the first laparoscopic surgery of a cholecystectomy. Since then numerous laparoscopic operations have been performed and there has been a lot of improvements and innovations in this field. Such surgical operations are characterised as **minimally invasive**, because the surgical incisions made at the patient are very small and thus the probability of infection of the patient during or after the operation are very small, the hospitalization time is reduced (which means mean better and more efficient use of hospital resources) and the overall recovery of the patient is significantly faster and less painful.

However, traditional laparoscopic mechanisms have some downsides as well. First of all, the surgeon should operate in a mirrored-way, meaning that they should move at the opposite direction from what they saw at the screen (this effect is also known as the **fulcrum effect**), in order to reach the desired point of operation. Earlier laparoscopic tools had less degrees of freedom, which means less flexibility in motion control. Moreover these systems provided limited touch sensibility and feedback to the doctor they were very susceptible to the surgeon's micro movements and tremble.

The first application of robotics in Surgery appears in 1985, when Kwoh et al. [46] used a **PUMA 560**, a standard industrial robotic arm, to perform a neurosurgical biopsy, where the biopsy needle was inserted in the brain and guided with the help of Computed Tomography. This successful application was followed by the **PROBOT** surgical robot [33], which was developed at the Imperial College and used in a prostatectomy operation. Another example of an early surgery robot was the **ROBODOC** system [6] developed by Integrated Surgical Supplies in Sacramento California, which was the first to be used in orthopedics for a hip replacement surgery and was also the first to be approved by the FDA (Food & Drug Administration, organization responsible for medical devices, drugs etc.).

Figure 1: The PUMA 560 robotic arm, which was the first to be used in surgery robotics in 1985

Some other important surgery robots are listed below:

- **AESOP®Endoscope Positioner**: A voice controlled endoscopic system
- **HERMES®Control Center**

- **daVinci Surgical System®**: One of the most popular surgery robots and most used in hospitals. It is a master-slave system, which means that the operation commands are sent unidirectionally from the master console, which is controlled by the surgeon, and are executed by the robot. It also comes with a high definition 3D video feed and advanced manipulator system, one for each hand, called EndoWrist®. It is officially approved by the FDA for laparoscopic surgeries.

- **SOCRATES Robotic Telecollaboration System**

- **Raven-II** [22]: An open platform for collaborative research on surgical robotics.

- **Monarch™Platform** by Auris Health Inc., an endoscopic system for robotic-assisted bronchoscopy

Figure 2: DaVinci Xi, ©2020 Intuitive Surgical, Inc. Patient Cart with the robotic arms that control the surgical tools

Figure 3: The Monarch™Platform endoscopic system [1]

1.1.2 Surgical Robotics Procedure

The robotic surgery procedure starts with total anesthesia of the patient. Then the surgeon makes small incisions at the anatomical region of interest, where the procedure will take place. Through these small incisions special tubes, called trocars, are mounted, through which the laparoscopic tools are inserted. After the patient is prepared and after the patient cart, which carries the robotic arms, is successfully positioned and callibrated, the surgeon sits on a console, from where they control they robot via special sensitive joysticks. The surgeon has vision access (often in 3D) to the surgical site via a small endoscopic camera and the video is displayed on the console. In some cases, the surgeon gets force feedback from the joysticks via haptic mechanisms. Haptic force feedback is very important for the doctor in order to have a better sense of the anatomy and the surgical site, and it has gained a lot of interest in the reasearch community.

[1] https://www.aurishealth.com/patients/robotic-bronchoscopy-patient-about-monarch-platform

Figure 4: DaVinci Xi ©2020 Intuitive Surgical, Inc. Surgeon Console [2]

1.1.3 Advantages & Disadvantages of Surgical robotics

Surgical robotics have a huge impact in Medicine and Healthcare in general. Some of the advantages are the following:

- **Minimally Invasive Procedures** which means
  - Smaller incisions
  - Less blood loss
  - Reduced risk of inpatient infection
  - Less pain
  - Faster patient recovery
- Increased **precision** and reduced human errors
  - Smooth and precise movements
  - Detection and correction of errors caused by hand tremble
- **No fulcrum effect** and intuitive manipulation of surgical tools
- **Haptic feedback**. This technology uses small mechanical forces and vibrations to give the user the sense of touch or force. Force feedback gives the ability to the surgeon to understand the mechanical properties of the tissue they operate on, such as resistance and elasticity, and thus distinguish between healthy from unhealthy tissue
- **Teleoperation** (currently in the same room only): the surgeon operates while they sit on a special **ergonomic** console, which makes the long procedures more comfortable and efficient.

[2]https://www.intuitive.com/en-us/about-us/press/press-resources

1.2 Problem statement

The goal of this thesis is to design the kinematic models and algorithms necessary for a robotic arm to detect, pick and manipulate a laparoscopic surgical tool. To achieve these goals the robotic arm must successfully do the following:

- Use computer vision to detect the scene and laparoscopic tools and with the help of stereoscopic vision, calculate the position and orientation of the center of mass of each tool, with respect to the universal reference frame

- Calculate the contact points on the tool, on which the fingers of the gripper will be placed, so that there is a firm grasp (force closure)

- Calculate the path from the tools' table to the surgical site table

- Calculate the trajectory that needs to be executed when the tool is inserted in the trocar. This is a special type of trajectory, because the motion is constrained and is known in the bibliography as a **Remote Center of Motion** (RCM) control. The constraint is that, at each time one point of the inserted tool must coincide with the RCM point (this point will also be referenced in this thesis as the center of the trocar, or the fulcrum reference frame point).

1.3 Bibliography Overview

1.4 Methodology & Approach

2 Robotic arm Kinematic Analysis

2.1 Robotic arm, DH parameters & Forward Kinematics

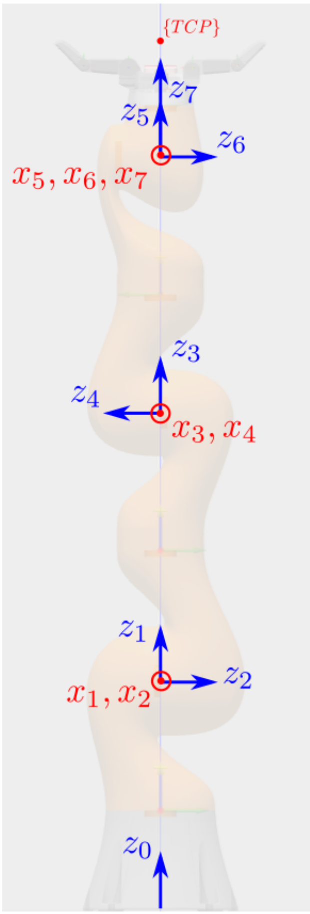

Figure 5: Joint reference frames of the KUKA iiwa14 robot

i	θ_i (rad)	L_{i-1} (m)	d_i (m)	α_{i-1} (rad)
1	θ_1	0	0.36	0
2	θ_2	0	0	$-\pi/2$
3	θ_3	0	0.36	$\pi/2$
4	θ_4	0	0	$\pi/2$
5	θ_5	0	0.4	$-\pi/2$
6	θ_6	0	0	$-\pi/2$
7	θ_7	0	0	$\pi/2$

$$
{}^{i-1}T_i = \begin{bmatrix} c\theta_i & -s\theta_i & 0 & L_{i-1} \\ s\theta_i c a_{i-1} & c\theta_i c a_{i-1} & -s a_{i-1} & -s a_{i-1} d_i \\ s\theta_i s a_{i-1} & c\theta_i s a_{i-1} & c a_{i-1} & c a_{i-1} d_i \\ 0 & 0 & 0 & 1 \end{bmatrix}
$$

2.2 Inverse Kinematics

2.2.1 Decoupling Technique

In this section the inverse kinematics problem is solved for only the 6 out of the 7 total degrees of freedom. The third joint is not used in this analysis and it's angle is set to zero $\theta_3 = 0$. The rest of the joints form a special kind of kinematic chain that can be solved using the decoupling technique. In this technique the Inverse kinematics problem is split to 2 separate subproblems, one for the position and one for the orientation of the end-effector. This technique can be applied in this case because the axes of the 3 last joints intersect at the same point and they form an Euler wrist.

To solve for the joints' angles, the transformation matrix ${}^0T_7$ of the end-effector with respect to the robot's base is required. Usually the transformation ${}^UT_{tcp}$ is known, which is the pose of Tool's center point (TCP) with respect to the Universal Coordinate Frame $\{U\}$ from which the required ${}^0T_7$ can be calculated

$$
{}^UT_{tcp} = {}^UT_0 \ {}^0T_7 \ {}^7T_{tcp}
$$

$$
{}^0T_7 = {}^UT_0^{-1} \ {}^UT_{tcp} \ {}^7T_{tcp}^{-1}
$$

$$
{}^0T_7 = \begin{bmatrix} R_t & \mathbf{p}_t \\ 0 & 1 \end{bmatrix}
$$

where ${}^UT_0$, ${}^7T_{tcp}$ are translation transformations by a constant distance and R_t, $\mathbf{p}_t$ are the target's orientation and position respectively.

$$
{}^0\mathbf{p}_5 = {}^0T_4 {}^4\mathbf{p}_5 = \begin{bmatrix} p_x \\ p_y \\ p_z \end{bmatrix}
$$

$$
\theta_1 = \begin{cases} atan2\,(p_y, p_x) \\ \pi - atan2\,(p_y, p_x) \end{cases} \tag{2.2.1}
$$

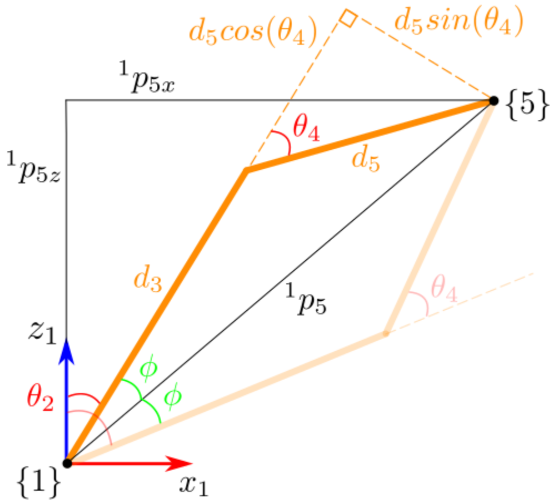

Figure 6: Calculation of angles θ_2, θ_4

$$\varphi = acos\left(\frac{d_3^2 + \|^1p_5\|^2 - d_5^2}{2d_3\|^1p_5\|}\right)$$

$$\theta_2 = atan2\left(\sqrt{p_x^2 + p_y^2}, {}^1p_{5z}\right) \pm \varphi \tag{2.2.2}$$

$$c_4 = \frac{\|^1p_5\|^2 - d_3^2 - d_5^2}{2d_3d_5}$$

$$\theta_4 = atan2\left(\pm\sqrt{1 - c_4^2}, c_4\right) \tag{2.2.3}$$

Once $\theta_1, \theta_2, \theta_3, \theta_4$ are known, the orientation matrix of the wrist can be calculated as following

$$R_{target} = \begin{bmatrix} i_x & j_x & k_x \\ i_y & j_y & k_y \\ i_z & j_z & k_z \end{bmatrix}$$

$$\theta_6 = atan2\left(\pm\sqrt{1 - k_y^2}, k_y\right) \tag{2.2.4}$$

$$\theta_7 = atan2\left(-j_y, i_y\right)$$

$$\theta_5 = atan2\left(-k_z, k_x\right)$$

2.2.2 Workspace constraints & Singularity points

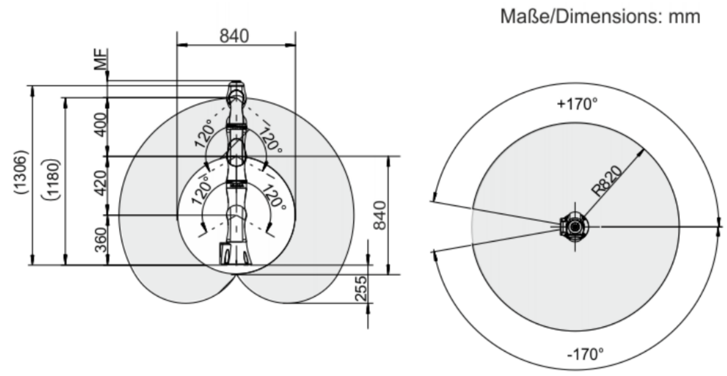

Figure 7: KUKA iiwa LBR14 workspace dimensions

Singularity points:

- When $p_x^2 + p_y^2 = 0$ then the end-effector lies on the z-axis and θ_1 is not defined
- When $sin\,(\theta_6) = 0$ then the angles θ_5, θ_7 are not defined

2.2.3 Solutions for 7DoF numerically

Jacobian

$$J = J(\mathbf{q}) = [J_1, J_2, \cdots, J_7] \in \mathbb{R}^{6\times 7}$$

$$J_i = \begin{bmatrix} {}^0\mathbf{z}_i \times ({}^0\mathbf{p}_8 - {}^0\mathbf{p}_i) \\ {}^0\mathbf{z}_i \end{bmatrix} \tag{2.2.5}$$

$J(\mathbf{q})$ is non rectangular and thus non-invertible. Instead of the inverse of the Jacobian the pseudoinverse is calculated which by the equation

$$J^\dagger = J^\top (JJ^\top)^{-1} \tag{2.2.6}$$

2.2.4 Comparison of Inverse Kinematics Techniques

3 Grasping

3.1 Gripper & Forward Kinematics

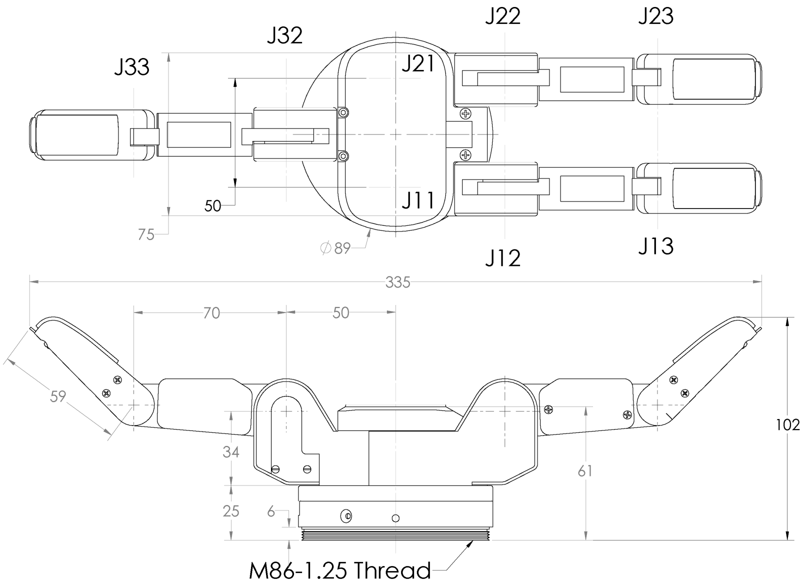

Figure 8: Barrett Hand gripper (model BH8-282) dimensions

3.2 Gripper Inverse Kinematics

The following Inverse Kinematics analysis referes to one finger of the Barrett Hand gripper, which has 3 revolute joints. Finger 3 has only 2 revolute joints for which the angle solutions are the same with the solutions of the last 2 joints of the other fingers. Let

$$\mathbf{p} = \begin{bmatrix} p_x \\ p_y \\ p_z \end{bmatrix}$$

be the position of the grasp point for one finger. The first angle can easily be calculated as

$$\varphi_1 = atan2\left(p_y, p_x\right) \tag{3.2.1}$$

Next, we calculate the third angle based on the law of cosines (see fig.)

$$cos\left(\pi - \varphi_3 - \frac{\pi}{4}\right) = \frac{L_2^2 + L_3^2 - p^2}{2L_2L_3}$$

$$cos\left(\varphi_3 + \frac{\pi}{4}\right) = \frac{p^2 - L_2^2 - L_3^2}{2L_2L_3}$$

$$\varphi_3 = atan2\left[\pm\sqrt{1 - \left(\frac{p^2 - L_2^2 - L_3^2}{2L_2L_3}\right)^2}, \frac{p^2 - L_2^2 - L_3^2}{2L_2L_3}\right] - \frac{\pi}{4} \tag{3.2.2}$$

In a more general case, the first argument of the $atan2$ function in the expression of φ_3 could also be negative, but in this case this second solution is rejected, because due to mechanical constraints, this angle can't be negative. After having calculated φ_3 we can calculate φ_2

$$tan\,(\psi + \varphi_2) = \frac{p_z}{\sqrt{p_x^2 + p_y^2}}$$

$$tan\,(\psi) = \frac{L_3 sin\left(\varphi_3 + \frac{\pi}{4}\right)}{L_2 + L_3 cos\left(\varphi_3 + \frac{\pi}{4}\right)}$$

$$\varphi_2 = atan2\left(pz, \sqrt{p_x^2 + p_y^2}\right) - atan2\left[L_3 sin\left(\varphi_3 + \frac{\pi}{4}\right), L_2 + L_3 cos\left(\varphi_3 + \frac{\pi}{4}\right)\right] \tag{3.2.3}$$

3.3 Force closure

The planar case, the spatial case & convex hull test.

3.4 Firm grasping algorithm & Force control

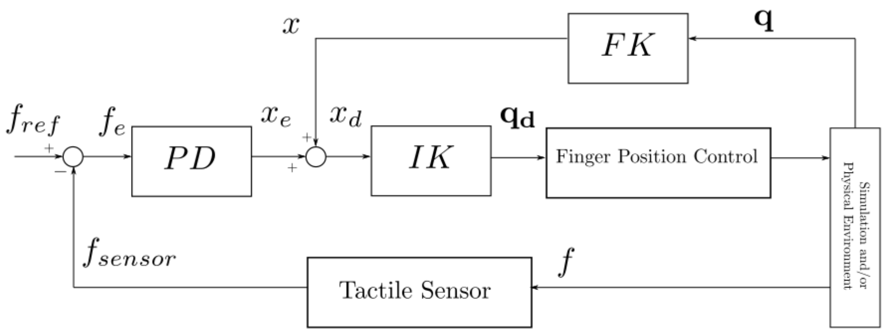

Figure 9: Force control on a Barrett Hand gripper finger

4 Scene and object recognition with Computer Vision

4.1 Laparoscopic tool detection

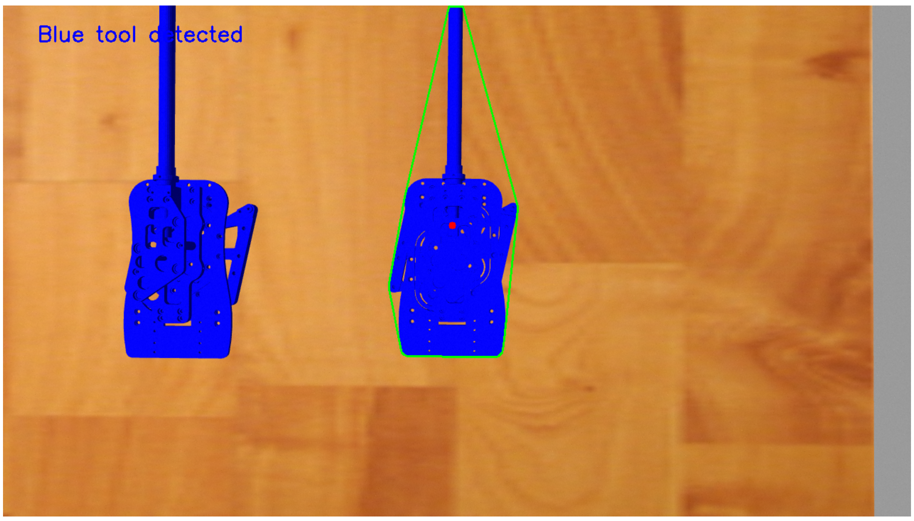

Figure 10: Simple tool detection in simulation based on color, using OpenCV. The green polygon is the convex hull, and the red point is the estimated center of mass

4.2 Stereoscopic vision

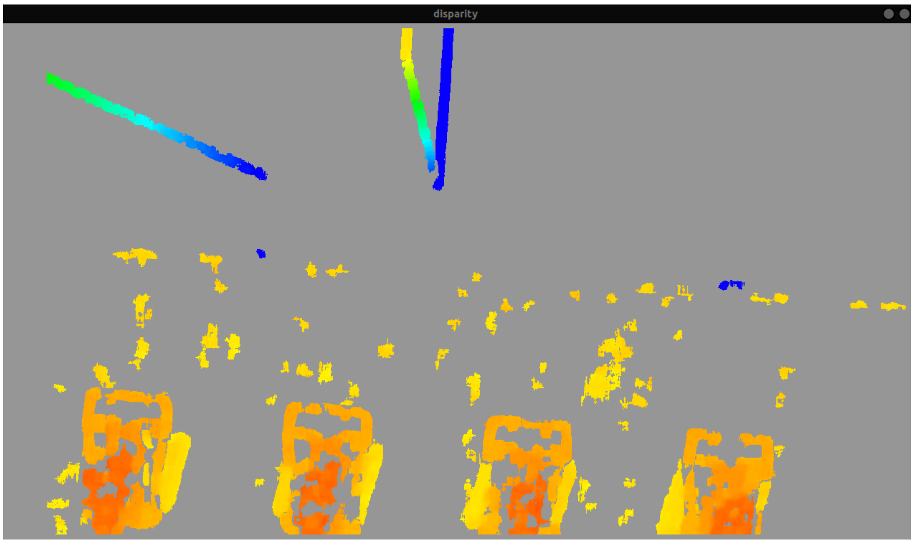

Figure 11: Disparity image calculated from the 2 cameras

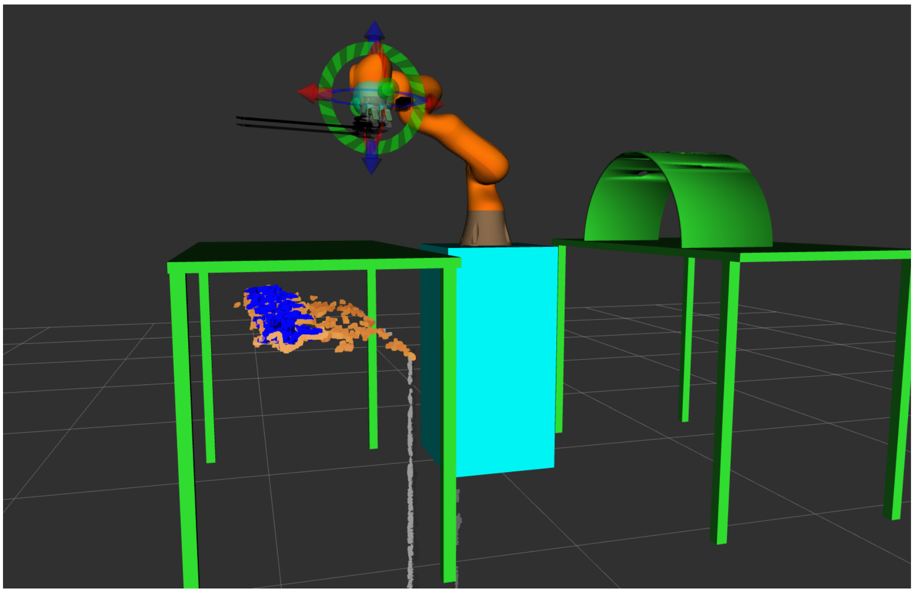

Figure 12: Point cloud of surgical tools, generated from the 2 cameras and visualized in RViz

4.3 Calculation of tool position and orientation

In order for the gripper to grasp correctly the laparoscopic tool, it is required to calculate the tool's position and orientation in the pixel space which must then be converted with respect to the robot's workspace. From all the pixels that have been classified as part of the laparoscopic tool, one can estimate the center of mass and two perpendicular vectors attached to that point that define the orientation. The center of mass is simply the average of the (x, y) coordinates of all the tool's pixels

$$(\bar{x}, \bar{y}) = \left(\frac{1}{N} \sum_{i=1}^{N} x_i, \frac{1}{N} \sum_{i=1}^{N} y_i \right)$$

The two orientation vectors are the eigenvectors of the covariance matrix of the above pixels. Let $\mathbf{a}, \mathbf{b}$ be the orientation vectors, then $\mathbf{a}, \mathbf{b}$ are solutions of the equation

$$C\mathbf{v} = \lambda\mathbf{v}$$

where C is the covariance matrix given by

$$C = \begin{bmatrix} \sigma(x,x) & \sigma(x,y) \\ \sigma(y,x) & \sigma(y,y) \end{bmatrix}$$

$$\sigma(x,y) = \frac{1}{n-1}\sum_{i=1}^{N}(x_i - \bar{x})(y_i - \bar{y})$$

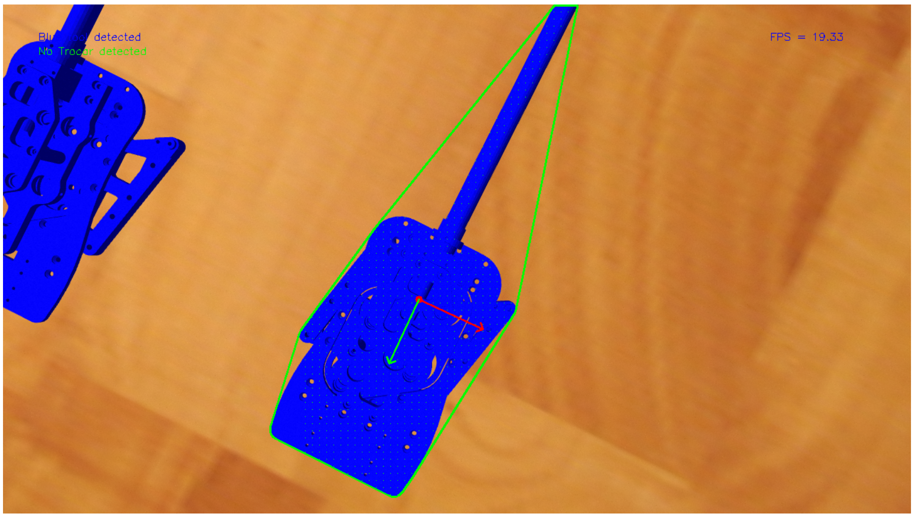

Figure 13: Estimation of tool's pose (position and orientation)

4.4 Calculation of grasping points

4.5 Trocar detection & Estimation of fulcrum point

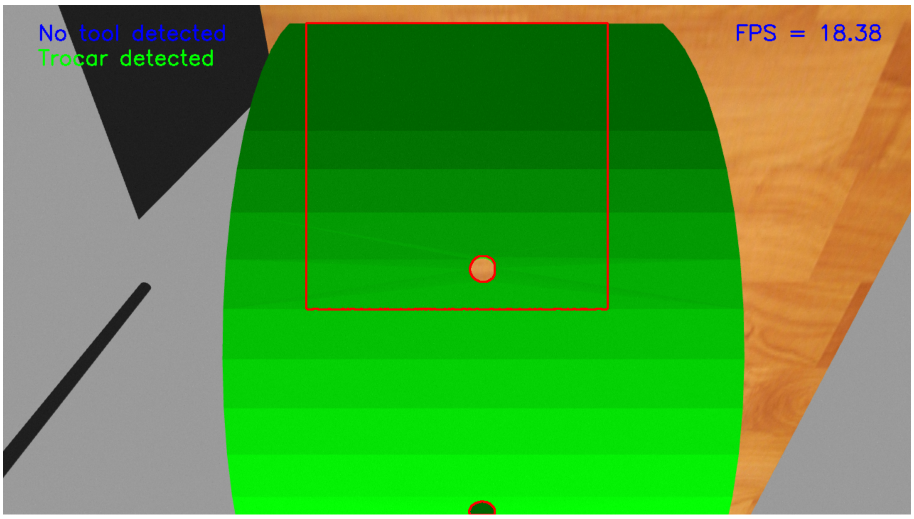

Figure 14: Simple trocar detection in simulation based on color, using OpenCV. In simulation, the trocar is simply considered to be a small cylindrical hole and it's center is the fulcrum point

5 Laparoscopic tool manipulation

5.1 Tool pose

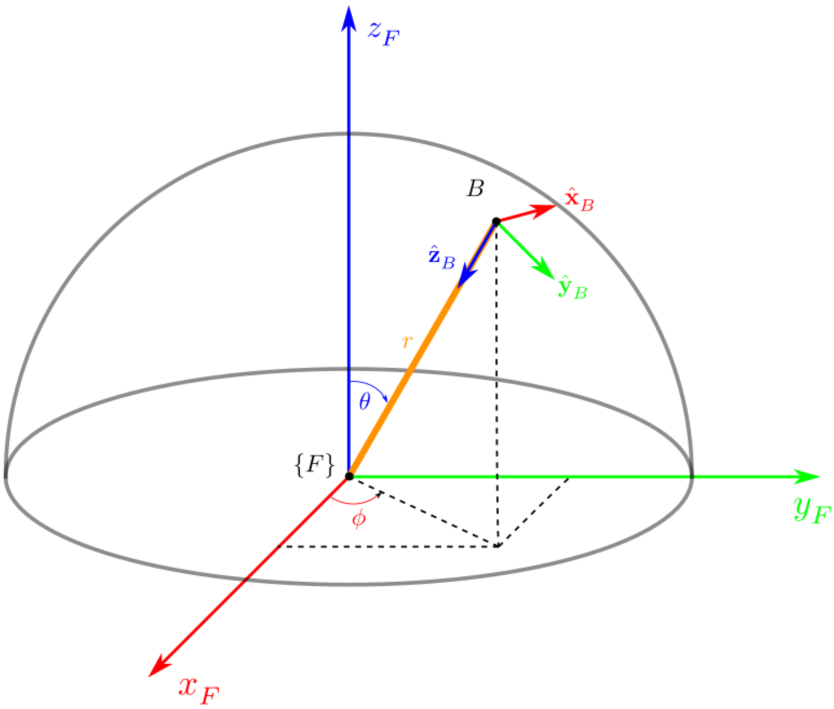

Figure 15: Tool pose at target point B calculated with respect to Fulcrum's reference frame $\{F\}$

The laparoscopic tool pose is given by the position and orientation vectors at target point B with respect to the coordinate frame $\{F\}$. The pose is given by the following transformation matrix

$$^F T_B = \begin{bmatrix} ^F R_B & ^F\mathbf{p}_B \\ \mathbf{0} & 1 \end{bmatrix} \quad where \quad ^F R_B = \begin{bmatrix} \hat{\mathbf{x}}_B & \hat{\mathbf{y}}_B & \hat{\mathbf{z}}_B \end{bmatrix}$$

$$\hat{\mathbf{x}}_B = \hat{\theta} = cos(\theta)cos(\varphi)\hat{\mathbf{x}}_F + cos(\theta)sin(\varphi)\hat{\mathbf{y}}_F - sin(\theta)\hat{\mathbf{z}}_F = \begin{bmatrix} cos(\theta)cos(\varphi) \\ cos(\theta)sin(\varphi) \\ -sin(\theta) \end{bmatrix}$$

$$\hat{\mathbf{y}}_B = \hat{\varphi} = -sin(\varphi)\hat{\mathbf{x}}_F + cos(\varphi)\hat{\mathbf{y}}_F = \begin{bmatrix} -sin(\varphi) \\ cos(\varphi) \\ 0 \end{bmatrix}$$

$$\hat{\mathbf{z}}_B = -\hat{\mathbf{r}} = -(sin(\theta)cos(\varphi)\hat{\mathbf{x}}_F + sin(\theta)sin(\varphi)\hat{\mathbf{y}}_F + cos(\theta)\hat{\mathbf{z}}_F) = \begin{bmatrix} -sin(\theta)cos(\varphi) \\ -sin(\theta)sin(\varphi) \\ -cos(\theta) \end{bmatrix}$$

The position of the point B is given in spherical coordinates by:

- $r = \rho$: outside penetration of laparoscopic tool
- $\theta = \beta$: altitude angle
- $\varphi = \alpha$: orientation angle

thus the position with respect to the coordinate frame $\{F\}$ is given by

$$^F\mathbf{p}_B = \begin{bmatrix} \rho sin(\beta)cos(\alpha) \\ \rho sin(\beta)sin(\alpha) \\ \rho cos(\beta) \end{bmatrix} = \rho\hat{\mathbf{r}}$$

The above goal point must be the same as the TCP point of the robot's end-effector. This means, that this pose must be converted with respect to the robot's reference frames.

$$^UT_{TCP} = {^UT_B}$$

$$^UT_0\,{^0T_7}\,{^7T_{TCP}} = {^UT_F}\,{^FT_B}$$

$$^0T_7 = {^UT_0^{-1}}\,{^UT_F}\,{^FT_B}\,{^7T_{TCP}^{-1}} \tag{5.1.1}$$

5.2 Pivoting motion with respect to Fulcrum Point

5.2.1 Circular trajectory of tool tip

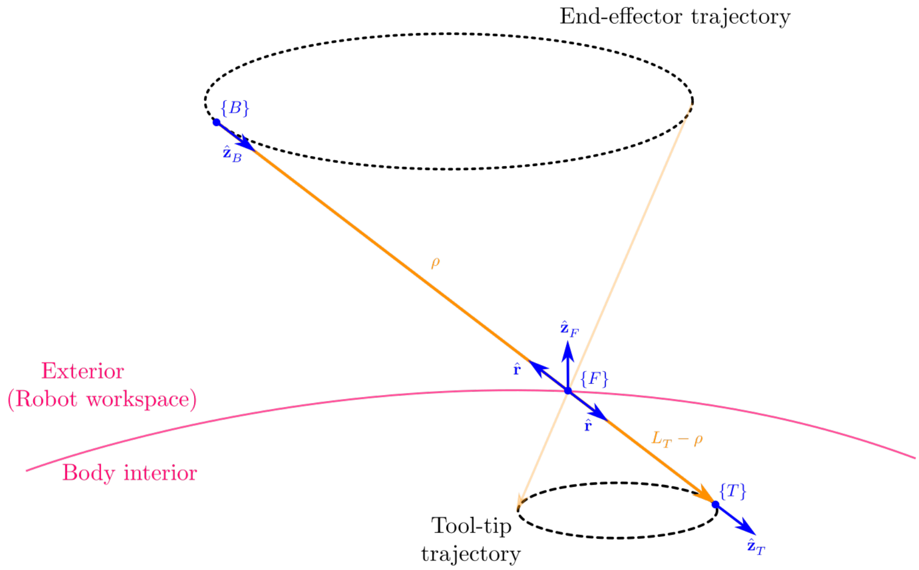

Figure 16: Circular trajectory of tool tip with respect to Fulcrum reference frame

To generate a circular trajectory for the pivot movement we must specify the center of the circle and a vector whose magnitude is the radius of the circle and it's direction gives the orientation of the plane that the circle lies at. The simplest case of a circular trajectory is the one, whose circle lies in a plane parallel to the xy plane.
We first consider the motion of the laparoscopic tool tip on a circle parallel to a z-plane, with respect to the $\{F\}$ coordinate frame.

$$(x_F - x_{F0})^2 + (y_F - y_{F0})^2 = r_0^2, \quad z_F = z_{F0}$$

It's often more convenient to express trajectories in a parametric form, which makes it easier to calculate all the waypoints of the trajectory

$$\begin{cases} x_F = r_0 cos(2\pi t) + x_{F0} \\ y_F = r_0 sin(2\pi t) + y_{F0} \\ z_F = z_{F0} \end{cases}, \quad t \in [0, 1]$$

After having calculated the cartesian coordinates we can calculate the spherical coordinates as follows

$$\begin{cases} r = \sqrt{x_F^2 + y_F^2 + z_F^2} \\ \theta = atan2\left(\sqrt{x_F^2 + y_F^2}, z_F\right) \\ \varphi = atan2(y_F, x_F) \end{cases} \tag{5.2.1}$$

5.2.2 Circular arc trajectory of tool tip

To generate a circular arc trajectory for a pivot motion we must specify the same parameters as in the circular trajectory as well as the length of the arc or the total angle of the arc section.

5.2.3 Line segment trajectory of tool tip

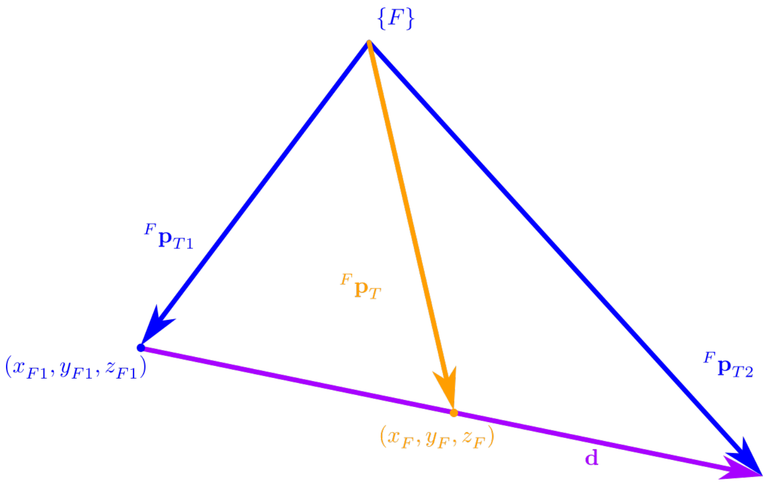

Figure 17: Line segment trajectory of tool tip with respect to Fulcrum reference frame

$$\mathbf{d} = {}^F\mathbf{p}_{T2} - {}^F\mathbf{p}_{T1} = [l, m, n]^\top$$
$${}^F\mathbf{p}_T = [x_F, y_F, z_F]^\top$$
$${}^F\mathbf{p}_T = {}^F\mathbf{p}_{T1} + t\mathbf{d}$$
$$t = \frac{x_F - x_{F1}}{l} = \frac{y_F - y_{F1}}{m} = \frac{z_F - z_{F1}}{n} \quad t \in [0, 1]$$
$$\begin{cases} x_F = tl + x_{F1} \\ y_F = tm + y_{F1} \\ z_F = tn + z_{F1} \end{cases}$$

After having calculated the cartesian coordinates we can calculate the spherical coordinates using the 5.2.1 equations.
The line segment trajectory of tool tip, as analysed in this section needs no implementation as it is already implemented in the ROS MoveIt library and can be used by calling the method **computeCartesianPath**.

5.3 Task space analysis

Dexterity analysis for tool's task space

$$\mathcal{D} = \mathcal{L}_q \mathcal{M} \tag{5.3.1}$$

where

$$\mathcal{M} = \sqrt{det(JJ^\top)} \tag{5.3.2}$$

$$\mathcal{L}_q = 1 - \exp\left\{ -\kappa \prod_{i=1}^{n_k} \frac{(q_i - q_{i,\min})(q_{i,\max} - q_i)}{(q_{i,\max} - q_{i,\min})^2} \right\} \tag{5.3.3}$$

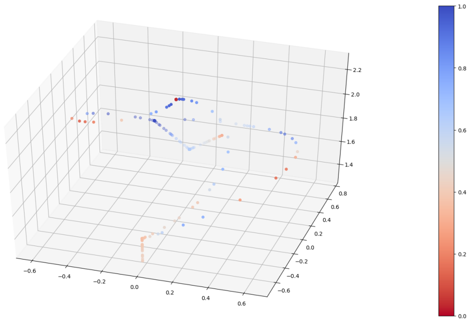

Figure 18: Plot the manipulability of the robot arm at sample points of the executed trajectory

For maximum dexterity at most points of a trajectory in a pivoting motion, the pivot sub- taskspace (i.e. the space of all configurations of feasible pivot motions) must be fully within the robot's whole reachable taskspace, otherwise only a small range of pivot movements will be feasible.

6 Path Planning

6.1 Path searching

Find path points (position and orientation) by avoiding collisions, asserting that path points is within robot's workspace and by avoiding singularity points.

6.2 Pick and place algorithm

7 Trajectory Planning

At this step, given the points of the desired path, a more detailed trajectory is calculated, which will contain all the waypoints that the robot will have to visit.

7.1 Trajectory planning in cartesian coordinates

Connect the points from path planning with line segments and add more points if needed

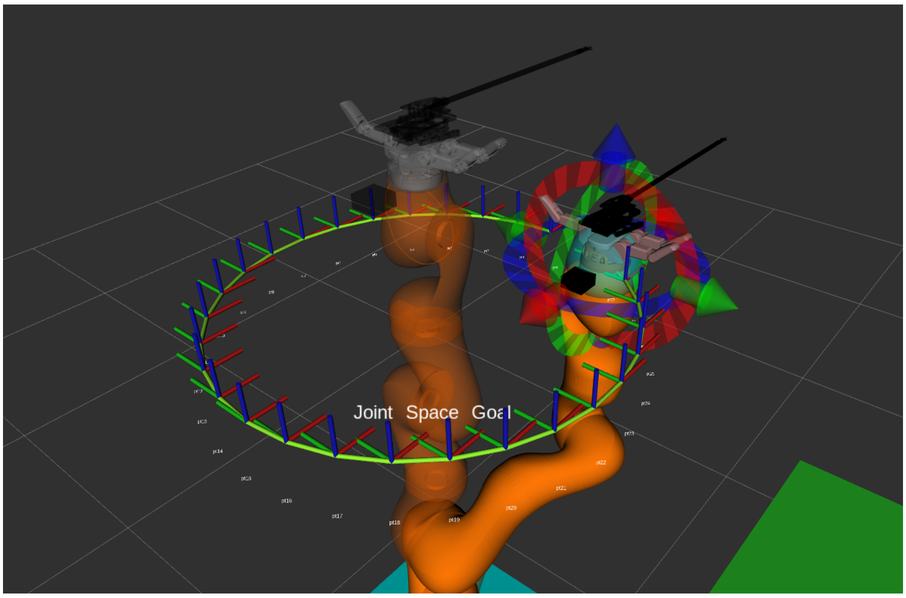

Figure 19: Circlular trajectory around the z axis of the home position of the robot

It is very important that the designed trajectory respects the joints angles' range. For example depending on the starting position of the circular trajectory depicted at figure 19, the robot arm may reach it's joint bounds and in order to continue executing the trajectory it will have to make a sudden jump to reset the angles. This could have serious side-effects for both the surgical task and thus the patient, as well as for the operating staff, who control the robot.

7.2 Trajectory planning in joint angles space

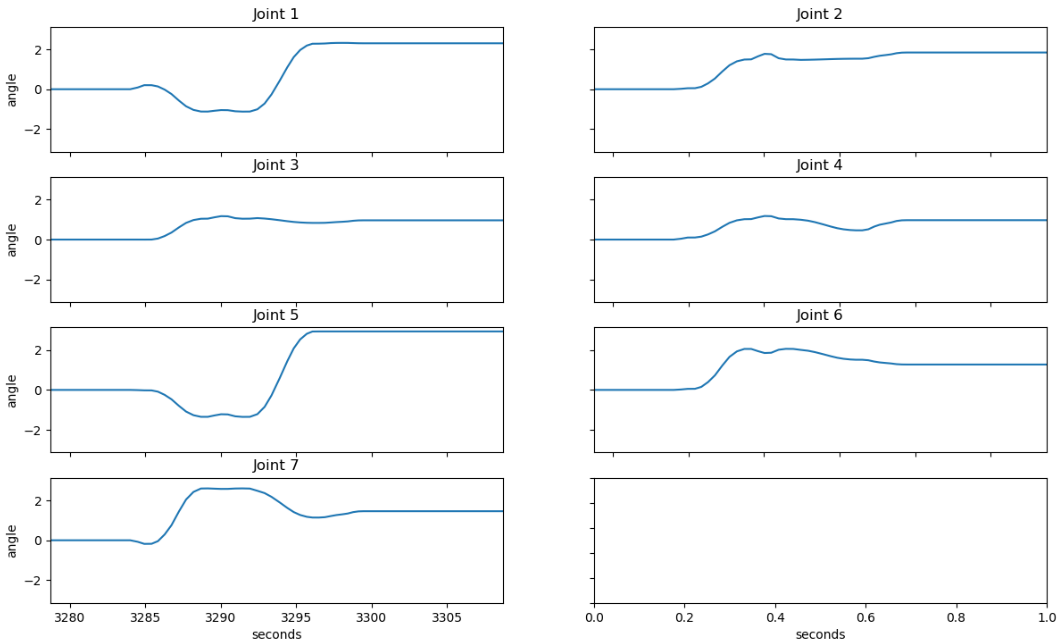

Figure 20: Trajectory diagrams in joints space.

8 Implementation with the ROS framework

8.1 Introduction to the ROS framework

ROS is an open-source robotics software framework. It is a meta-operating system, which means that it provides its own abstractions on top of the host's operating system including filesystem, hardware abstractions, low-level device control, package management and networking. It also provides tools and services to develop large, scalable robotics software, it supports a wide variety of libraries and programming languages and it has a huge community, support and documentation resources.

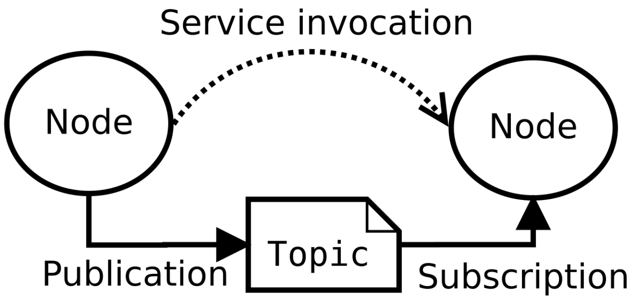

Figure 21: Communication diagram of 2 ROS nodes with a topic and a service

8.2 Gazebo simulation environment

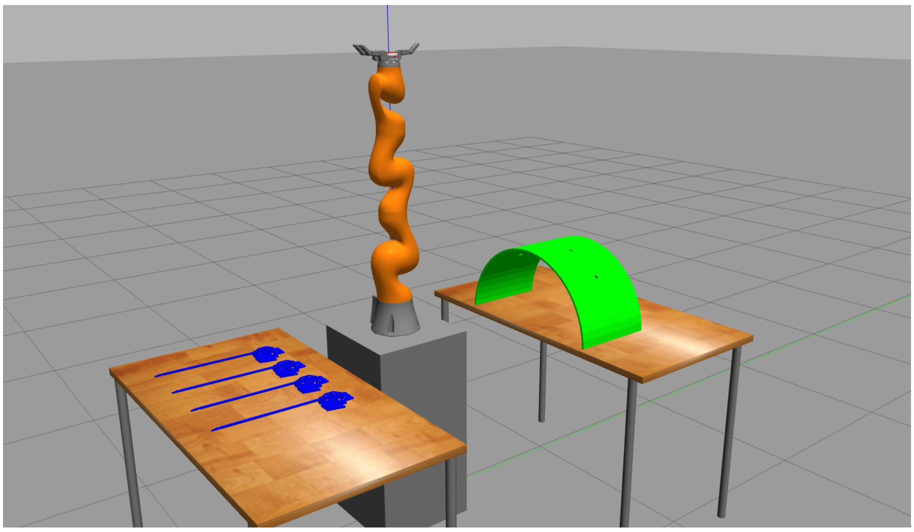

Figure 22: Simulation environment in Gazebo

The main environment setup of this thesis was designed using the Gazebo simulation environment and it consists of the following objects:

- the robot arm, KUKA®iiwa14 lbr, being at the center of the setup
- the robot base, so that the robot arm can better reach the tools and the surgical site and have more flexibility in movment
- 2 tables, one for the tools and one for the surgical site

- 4 surgical tools, using a modified version of the surgical tools used in the Raven II surgical platform
- a mounting dock, which has holes that have the same role as the trocars (small tubes from which the surgical tool is inserted). Initially a mounting dock with 4 same holes of 4mm diameter was used, but it was later replaced with a new one with holes of variable diameters to test feasibility of pivot motions. Larger diameters means more space for motion planner to search for solution and thus more probable to find a solution.

8.3 Visualization and Motion Planning with RViz and Moveit

Motion Planning parameters outside of body:

- Position tolerance: 50µm
- Orientation tolerance: 0.00005 deg
- Planning time: 10s

Motion Planning parameters inside of body:

- Position tolerance:
- Orientation tolerance:
- Planning time
- End-effector interpolation step: 1mm
- Maximum velocity scaling factor

Sometimes the motion planner finds a solution but the execution from the controller is aborted. After many iterations of the same experiment this does not happen always, which means that the feasibility of the execution of the movement by the controller depends on the initial state of the robot, i.e. if initially some joints of the robot are at their boundaries, then the next commanded trajectory maybe unfeasible.
At each time step it is important to publish a custom message containing all the information about the kinematic state of the robot. In this thesis a custom **ROS** message was created containing a tf transform with a 3D vector for the position and a quaternion for the rotation and a custom 6-by-7 matrix containing the values of the Jacobian. The MoveIt library, from which the kinematic state of the robot is obtained, returns the orientation of the end effector as a 3-by-3 rotation matrix, but in the ROS tf message it must be expressed as a quaternion. To convert the matrix to a quaternion we first calculate the euler angles and then use these values to construct the quaternion "vector". The quaternion representation of rotation is often preferred in robotic applications due to its efficiency in calculations and memory. To convert the transformation matrix to euler angles and then to quaternions the following formulas were used:

$$T = \begin{bmatrix} r_{11} & r_{12} & r_{13} & x \\ r_{21} & r_{22} & r_{23} & y \\ r_{31} & r_{32} & r_{33} & z \\ 0 & 0 & 0 & 1 \end{bmatrix}$$

$$\varphi = atan2(r_{21}, r_{11})$$

$$\theta = atan2(-r_{31}, \sqrt{r_{11}^2 + r_{21}^2})$$

$$\psi = atan2(r_{32}, r_{33})$$

where T is the transformation matrix and φ, θ, ψ are the roll, pitch and yaw (Euler) angles.

8.4 Experiments and Development methodology

8.4.1 Robot Planner 1

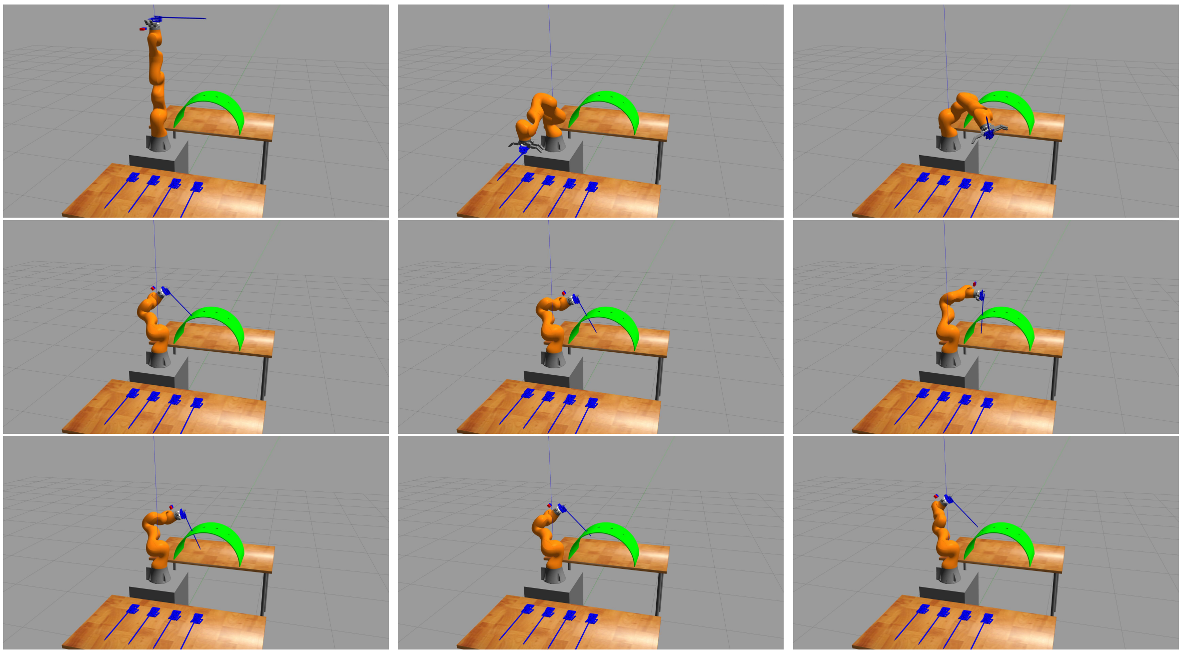

Figure 23: Experiment 1:

8.4.2 Robot Planner 2

8.4.3 Robot Planner 3

8.4.4 Robot Planner 4

8.4.5 Robot Planner 5

9 Results and Future Work

9.1 Results

9.2 Conclusions & Comparison with similar projects

9.3 Future Work

Nomenclature

$\hat{\mathbf{r}}, \hat{\boldsymbol{\theta}}, \hat{\boldsymbol{\phi}}$ Unit vectors of r, θ, φ axes respectively, in spherical coordinates

$\hat{\mathbf{x}}, \hat{\mathbf{y}}, \hat{\mathbf{z}}$ Unit vectors of x, y, z axes respectively

$\mathcal{L}_q$ Dexterity measure of the robotic arm

$\mathcal{M}$ Manipulability measure of the robotic arm

${}^{i-1}\mathbf{p}_{iO}$ Position vector from the origin of the coordinate frame $\{i\}$ to the origin of the coordinate frame $\{i-1\}$

${}^{i-1}R_i$ Rotation matrix from coordinate frame $\{i\}$ to coordinate frame $\{i-1\}$

${}^{i-1}T_i$ Transformation matrix from coordinate frame $\{i\}$ to coordinate frame $\{i-1\}$

c_i Shorthand notation for $cos\theta_i$

$J^\dagger$ Pseudoinverse of the Jacobian

s_i Shorthand notation for $sin\theta_i$

List of Figures

List of programs

Bibliography

[1] Nastaran Aghakhani et al. "Task control with remote center of motion constraint for minimally invasive robotic surgery". In: *2013 IEEE International Conference on Robotics and Automation* (2013), pp. 5807–5812.

[2] E. Bauzano et al. "Active wrists endoscope navigation in robotized laparoscopic surgery". In: *2009 IEEE International Conference on Mechatronics*. Apr. 2009, pp. 1–6. DOI: 10.1109/ICMECH.2009.4957177.

[3] E. Boctor et al. "Virtual Remote Center of Motion Control for Needle Placement Robots". In: *Computer aided surgery : official journal of the International Society for Computer Aided Surgery* 9 5 (2003), pp. 175–83.

[4] M. C. Capolei et al. "Positioning the laparoscopic camera with industrial robot arm". In: *2017 3rd International Conference on Control, Automation and Robotics (ICCAR)*. Apr. 2017, pp. 138–143. DOI: 10.1109/ICCAR.2017.7942675.

[5] Sachin Chitta et al. "ros_control: A generic and simple control framework for ROS". In: *The Journal of Open Source Software* (2017). DOI: 10.21105/joss.00456. URL: http://www.theoj.org/joss-papers/joss.00456/10.21105.joss.00456.pdf.

[6] G. Cowley. "Introducing "Robodoc". A robot finds his calling–in the operating room". In: *Newsweek* 120.21 (Nov. 1992), p. 86.

[7] Bassem Dahroug, B. Tamadazte, and N. Andreff. "3D Path Following with Remote Center of Motion Constraints". In: *ICINCO*. 2016.

[8] Bassem Dahroug, B. Tamadazte, and N. Andreff. "Task Controller for Performing Remote Centre of Motion". In: *ICINCO*. 2016.

[9] Bassem Dahroug, B. Tamadazte, and N. Andreff. "Visual servoing controller for time-invariant 3D path following with remote centre of motion constraint". In: *2017 IEEE International Conference on Robotics and Automation (ICRA)* (2017), pp. 3612–3618.

[10] Bassem Dahroug, Brahim Tamadazte, and Nicolas Andreff. "Unilaterally Constrained Motion of a Curved Surgical Tool". In: *Robotica* (2020), pp. 1–23. DOI: 10.1017/S0263574719001735.

[11] M. M. Dalvand and B. Shirinzadeh. "Remote centre-of-motion control algorithms of 6-RRCRR parallel robot assisted surgery system (PRAMiSS)". In: *2012 IEEE International Conference on Robotics and Automation* (2012), pp. 3401–3406.

[12] Carlos Faria et al. "Position-based kinematics for 7-DoF serial manipulators with global configuration control, joint limit and singularity avoidance". In: *Mechanism and Machine Theory* 121 (2018), pp. 317–334. ISSN: 0094-114X. DOI: https://doi.org/10.1016/j.mechmachtheory.2017.10.025. URL: http://www.sciencedirect.com/science/article/pii/S0094114X17306559.

[13] Tully Foote. "tf: The transform library". In: *Technologies for Practical Robot Applications (TePRA), 2013 IEEE International Conference on*. Open-Source Software workshop. Apr. 2013, pp. 1–6. DOI: 10.1109/TePRA.2013.6556373.

[14] K. Fujii et al. "Gaze contingent cartesian control of a robotic arm for laparoscopic surgery". In: *2013 IEEE/RSJ International Conference on Intelligent Robots and Systems*. Nov. 2013, pp. 3582–3589. DOI: 10.1109/IROS.2013.6696867.

[15] M. Fujii et al. "Relationship between workspace reduction due to collisions and distance between endoscope and target organ in pediatric endoscopic surgery". In: *5th IEEE RAS/EMBS International Conference on Biomedical Robotics and Biomechatronics*. Aug. 2014, pp. 46–51. DOI: 10.1109/BIOROB.2014.6913750.

[16] J. Funda et al. "Constrained Cartesian motion control for teleoperated surgical robots". In: *IEEE Trans. Robotics Autom.* 12 (1996), pp. 453–465.

[17] J. Funda et al. "Control and evaluation of a 7-axis surgical robot for laparoscopy". In: *Proceedings of 1995 IEEE International Conference on Robotics and Automation*. Vol. 2. 1995, 1477–1484 vol.2.

[18] Alessandro Gasparetto et al. "Path Planning and Trajectory Planning Algorithms: A General Overview". In: *Motion and Operation Planning of Robotic Systems: Background and Practical Approaches*. Ed. by Giuseppe Carbone and Fernando Gomez-Bravo. Cham: Springer International Publishing, 2015, pp. 3–27. ISBN: 978-3-319-14705-5. DOI: 10.1007/978-3-319-14705-5_1. URL: https://doi.org/10.1007/978-3-319-14705-5_1.

[19] G. Gras et al. "Implicit gaze-assisted adaptive motion scaling for highly articulated instrument manipulation". In: *2017 IEEE International Conference on Robotics and Automation (ICRA)*. May 2017, pp. 4233–4239. DOI: 10.1109/ICRA.2017.7989488.

[20] Techbriefs Media Group. *Surgical Robotics: The Evolution of a Medical Technology - Medical Design Briefs*. URL: https://www.medicaldesignbriefs.com/component/content/article/mdb/features/technology-leaders/25006 (visited on 09/18/2020).

[21] G. B. Hanna, S. Shimi, and A. Cuschieri. "Optimal port locations for endoscopic intracorporeal knotting". In: *Surgical Endoscop* 11.4 (Apr. 1997), pp. 397–401. ISSN: 1432-2218. DOI: 10.1007/s004649900374. URL: https://doi.org/10.1007/s004649900374.

[22] B. Hannaford et al. "Raven-II: An Open Platform for Surgical Robotics Research". In: *IEEE Transactions on Biomedical Engineering* 60.4 (Apr. 2013), pp. 954–959. ISSN: 1558-2531. DOI: 10.1109/TBME.2012.2228858.

[23] M. R. Hasan et al. "Modelling and Control of the Barrett Hand for Grasping". In: *2013 UKSim 15th International Conference on Computer Modelling and Simulation*. Apr. 2013, pp. 230–235. DOI: 10.1109/UKSim.2013.142.

[24] Felix C. Huang et al. "Learning kinematic mappings in laparoscopic surgery". In: *Conference proceedings : ... Annual International Conference of the IEEE Engineering in Medicine and Biology Society. IEEE Engineering in Medicine and Biology Society. Annual Conference* 2010 (2010). PMC3280950[pmcid], pp. 2097–2102. ISSN: 1557-170X. DOI: 10.1109/IEMBS.2010.5626188. URL: https://pubmed.ncbi.nlm.nih.gov/21095685.

[25] J. Hutzl and H. Wörn. "Spatial probability distribution for port planning in minimal invasive robotic surgery (MIRS)". In: *2015 6th International Conference on Automation, Robotics and Applications (ICARA)*. Feb. 2015, pp. 204–210. DOI: 10.1109/ICARA.2015.7081148.

[26] Reza N. Jazar. *Theory of Applied Robotics, Kinematics, Dynamics, and Control (2nd Edition)*. Springer, Boston, MA, 2010. ISBN: 978-1-4419-1750-8. DOI: 10.1007/978-1-4419-1750-8.

[27] Abbas Karami et al. "Force, orientation and position control in redundant manipulators in prioritized scheme with null space compliance". In: *Control Engineering Practice* 85 (2019), pp. 23–33.

[28] I. Kuhlemann et al. "Robust inverse kinematics by configuration control for redundant manipulators with seven DoF". In: *2016 2nd International Conference on Control, Automation and Robotics (ICCAR)*. Apr. 2016, pp. 49–55. DOI: 10.1109/ICCAR.2016.7486697.

[29] P. Lago, Carlo Lombardi, and I. Vallone. "From laparoscopic surgery to 3-D double console robot-assisted surgery". In: *Proceedings of the 10th IEEE International Conference on Information Technology and Applications in Biomedicine* (2010), pp. 1–4.

[30] Kevin M Lynch and Frank C. Park. *Modern Robotics: Mechanics, Planning, and Control*. English (US). Cambridge Univeristy Press, 2017. ISBN: 978-1107156302.

[31] M. Marinho et al. "A Unified Framework for the Teleoperation of Surgical Robots in Constrained Workspaces". In: *2019 International Conference on Robotics and Automation (ICRA)* (2019), pp. 2721–2727.

[32] Murilo M. Marinho, Mariana C. Bernardes, and Antônio Padilha Lanari Bo. "A programmable remote center-of-motion controller for minimally invasive surgery using the dual quaternion framework". In: *5th IEEE RAS/EMBS International Conference on Biomedical Robotics and Biomechatronics* (2014), pp. 339–344.

[33] Q. Mei et al. "PROBOT — A computer integrated prostatectomy system". In: *Visualization in Biomedical Computing*. Ed. by Karl Heinz Höhne and Ron Kikinis. Berlin, Heidelberg: Springer Berlin Heidelberg, 1996, pp. 581–590. ISBN: 978-3-540-70739-4.

[34] Victor F. Muñoz et al. "Pivoting motion control for a laparoscopic assistant robot and human clinical trials". In: *Advanced Robotics* 19 (2005), pp. 694–712.

[35] A. A. Navarro et al. "Automatic positioning of surgical instruments in minimally invasive robotic surgery through vision-based motion analysis". In: *2007 IEEE/RSJ International Conference on Intelligent Robots and Systems*. Oct. 2007, pp. 202–207. DOI: 10.1109/IROS.2007.4399150.

[36] Jason M. O'Kane. *A Gentle Introduction to ROS*. Available at http://www.cse.sc.edu/~jokane/agitr/. Independently published, Oct. 2013. ISBN: 978-1492143239.

[37] Claudio Pacchierotti. "Needle Insertion in Simulated Soft Tissue". In: *Cutaneous Haptic Feedback in Robotic Teleoperation*. Cham: Springer International Publishing, 2015, pp. 21–36. ISBN: 978-3-319-25457-9. DOI: 10.1007/978-3-319-25457-9_2. URL: https://doi.org/10.1007/978-3-319-25457-9_2.

[38] Jaydeep Palep. "Robotic assisted minimally invasive surgery". In: *Journal of minimal access surgery* 5 (Feb. 2009), pp. 1–7. DOI: 10.4103/0972-9941.51313.

[39] C. Pham et al. "Analysis of a moving remote center of motion for robotics-assisted minimally invasive surgery". In: *2015 IEEE/RSJ International Conference on Intelligent Robots and Systems (IROS)* (2015), pp. 1440–1446.

[40] M. Quigley. "ROS: an open-source Robot Operating System". In: *ICRA 2009*. 2009.

[41] Morgan Quigley et al. "ROS: an open-source Robot Operating System". In: *ICRA Workshop on Open Source Software*. 2009.

[42] S. Roh et al. "Development of the SAIT single-port surgical access robot slave arm based on RCM Mechanism". In: *2015 37th Annual International Conference of the IEEE Engineering in Medicine and Biology Society (EMBC)* (2015), pp. 5285–5290.

[43] *ROS/Concepts - ROS Wiki*. URL: https://wiki.ros.org/ROS/Concepts (visited on 09/19/2020).

[44] Benoît Rosa et al. "Estimation of optimal pivot point for remote center of motion alignment in surgery". In: *International Journal of Computer Assisted Radiology and Surgery* 10.2 (Feb. 2015), pp. 205–215. ISSN: 1861-6429. DOI: 10.1007/s11548-014-1071-3. URL: https://doi.org/10.1007/s11548-014-1071-3.

[45] Hamid Sadeghian, Fatemeh Zokaei, and Shahram Hadian Jazi. "Constrained Kinematic Control in Minimally Invasive Robotic Surgery Subject to Remote Center of Motion Constraint". In: *Journal of Intelligent & Robotic Systems* (2019), pp. 1–13.

[46] H. Shao et al. "A New CT-Aided Robotic Stereotaxis System". In: 1985.

[47] I. A. Şucan and S. Chitta. *Moveit!* URL: https://moveit.ros.org/ (visited on 04/28/2020).

[48] V. Vitiello et al. "Emerging Robotic Platforms for Minimally Invasive Surgery". In: *IEEE Reviews in Biomedical Engineering* 6 (2013), pp. 111–126.

[49] Go Watanabe, ed. *Robotic Surgery*. Springer Japan, 2014. DOI: 10.1007/978-4-431-54853-9. URL: https://doi.org/10.1007/978-4-431-54853-9.

[50] Haiwang Xu et al. "Laparoscopic Robot Design and Kinematic Validation". In: Jan. 2007, pp. 1426–1431. DOI: 10.1109/ROBIO.2006.340138.

[51] Tao Yang et al. "Mechanism of a Learning Robot Manipulator for Laparoscopic Surgical Training". In: *Intelligent Autonomous Systems 12*. Ed. by Sukhan Lee et al. Berlin, Heidelberg: Springer Berlin Heidelberg, 2013, pp. 17–26. ISBN: 978-3-642-33932-5.

[52] L. Yu et al. “Research on the Trajectory Planning of the Minimally Invasive Surgical Robot 6-DOF Manipulator”. In: *2010 International Conference on Biomedical Engineering and Computer Science*. Apr. 2010, pp. 1–4. DOI: 10.1109/ICBECS.2010.5462451.

[53] Xiaoqin Zhou et al. “New remote centre of motion mechanism for robot-assisted minimally invasive surgery”. In: *BioMedical Engineering OnLine* 17 (2018).